

# Sensitivity of the SPIRE Detectors to Operating Parameters

**Document Number: SPIRE-UCF-DOC-002901**

**Issue 1.0**

**November 14 2007**

**Matt Griffin**

## Contents

1.	Introduction .....	2
2.	List of symbols .....	2
3.	Principles of semiconductor bolometers.....	3
4.	Bolometer model .....	3
4.1	The ideal thermal bolometer.....	3
4.2	Absolute calibration of the absorbed power.....	4
4.3	Typical parameters for the SPIRE bolometers .....	5
5.	Sensitivity of bolometer output and responsivity to operating parameters.....	7
5.1	Sensitivity to bath temperature.....	8
5.2	Sensitivity to background power .....	9
5.3	Sensitivity to signal power .....	11
5.4	Sensitivity to bias voltage.....	12
5.5	Relationship between responsivity and operating point voltage .....	13
6.	References .....	13

## 1. Introduction

This note assesses the sensitivity of the SPIRE bolometers to changes in their operating parameters (bath temperature, background power, bias voltage, signal power). A model of a typical PMW detector is used as an example. The results are discussed in terms of the variations expected in flight.

## 2. List of symbols

Symbol	Definition
$G_S$	Static thermal conductance between bolometer and heat sink
$G_d$	Dynamic thermal conductance between bolometer and heat sink
$I_{b-RMS}$	RMS bias current
$k$	Thermal conductivity of the link between the absorber and the heat sink
$P$	Electrical power dissipated in the bolometer
$Q$	Radiant power
$Q_B$	Background power absorbed by a bolometer
$Q_S$	Radiant power from the astronomical source absorbed by a bolometer
$R_d$	Detector resistance
$R_L$	Total load resistance
$R_S$	Bolometer resistance parameter
$S_o$	DC responsivity
$T$	Bolometer temperature
$T_g$	Bolometer material band-gap temperature
$T_o$	Bolometer heat sink temperature
$V_{b-RMS}$	RMS bias voltage
$V_{d-RMS}$	RMS voltage across detector
$V_S$	Decrease in RMS detector voltage at the operating point due to the astronomical signal
$W$	Total power dissipated in the bolometer
$Z_d$	Bolometer dynamic impedance at the operating point
$\beta$	Bolometer thermal conductivity power law index
$\phi$	Bolometer temperature normalised to the bath temperature
$\tau_{eff}$	Effective time constant (describes variation of responsivity with modulation frequency)
$\omega_s$	Signal frequency

### 3. Principles of semiconductor bolometers

The SPIRE detectors are semiconductor bolometers. The basic principles of operation are illustrated in Figure 1a.

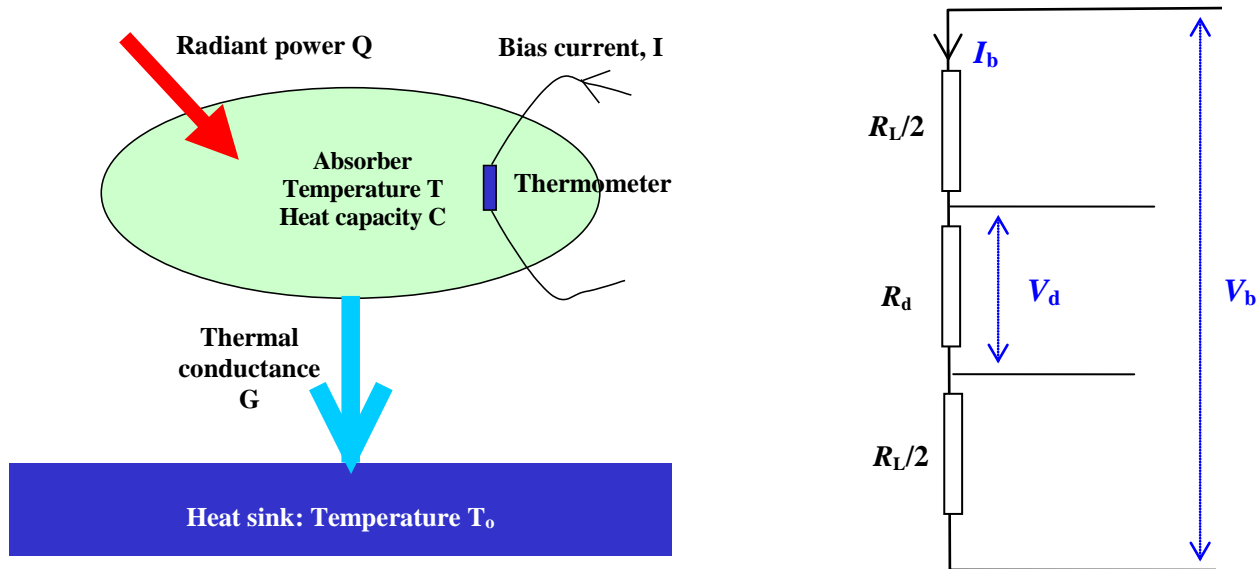


Figure 1: (a) Principle of bolometer operation; (b) bias circuit as used in SPIRE.

The bolometer comprises a low heat capacity absorber designed to absorb the incident submillimetre radiation. The absorber is coupled to a heat sink at a fixed temperature  $T_0$  by a thermal conductance,  $G$ . A semiconductor thermometer of resistance  $R_d$ , which depends on temperature, is attached to the absorber. A bias current, is passed throughout the thermometer, and the corresponding voltage across the thermometer is measured. Figure 1b shows the bias circuit used in SPIRE. The bolometer is biased (heated to its optimum operating temperature of around  $1.3T_0$ ) by applying a bias voltage across the chain formed by the bolometer and the two load resistors each with resistance  $R_L/2$ . In the case of SPIRE, the bias is provided as an AC excitation at a frequency too high for the bolometer thermal response to follow. The RMS detector current is  $I_{b-RMS} = V_{b-RMS}/(R_L + R_d)$ , which dissipates electrical power  $P = I_{b-RMS}^2 R_d$ , and thereby heats the bolometer to an operating temperature  $T$ , somewhat higher than  $T_0$ . Absorbed radiant power,  $Q$ , is thermalised in the absorber resulting in a further increase in  $T$  over the equilibrium value in the absence of illumination.

### 4. Bolometer model

#### 4.1 The ideal thermal bolometer

The SPIRE detectors can be accurately modelled as ideal thermal bolometers, based on the model of Mather as codified by Sudiwala *et al.* (2002). Here we list the main parameters that are used to characterise how the bolometer output varies as a function of operating temperature, bias, and optical loading.

For an NTD germanium bolometer, the resistance,  $R_d$ , depends only on its temperature and is given by

$$R_d(T) = R_S \exp \left[ \left( \frac{T_g}{T} \right)^{1/2} \right], \quad (1)$$

where  $T_g$  is a constant for the material and  $R_S$  is a constant for the particular device.

Assume for the moment that the bolometer is in a steady state condition at temperature  $T$ , with total power dissipation  $W$  having two contributions: RMS electrical power dissipation  $P$  and absorbed optical power  $Q$ :

$$W = P + Q. \quad (2)$$

The static thermal conductance,  $G_S$  is defined as

$$G_S = \frac{W}{T - T_o}, \quad (3)$$

and the dynamic thermal conductance is defined as

$$G_d = \frac{dW}{dT}. \quad (4)$$

The temperature variation of the thermal conductivity of the link to the heat sink is given by a power law with index  $\beta$ :

$$k(T) = k(T_o) \left[ \frac{T}{T_o} \right]^\beta = k(T_o) \phi^\beta, \quad (5)$$

where

$$\phi = \frac{T}{T_o}. \quad (6)$$

The static and dynamic thermal conductances are only equal at  $T = T_o$ :

$$G_d(T_o) = G_S(T_o) = G(T_o). \quad (7)$$

In general

$$G_S(\phi) = G(T_o) \left[ \frac{\phi^\beta - 1}{(\beta + 1)(\phi + 1)} \right]. \quad (8)$$

## 4.2 Absolute calibration of the absorbed power

If the bolometer parameters are known, then measurements of the RMS bolometer voltage and current can be used to determine the absolute absorbed power as follows:

$$P = V_d I_{b-RMS}, \quad (9)$$

$$R_d = \frac{V_{d-RMS}}{I_{b-RMS}}, \quad (10)$$

$$T = \frac{T_g}{\left[ \ln\left(\frac{R_d}{R_S}\right) \right]^2}, \quad (11)$$

$$\phi = \frac{T}{T_o}, \quad (12)$$

$$G_S(T) = G(T_o) \left[ \frac{\phi^\beta - 1}{(\beta + 1)(\phi + 1)} \right], \quad (12)$$

$$Q = G_S(T)[T - T_o] - P. \quad (13)$$

For most bolometer instruments, this absolute calibration is not normally attempted as part of the standard data reduction scheme. The common practice is to determine, by means of calibration observations of astronomical standards, the overall responsivity of the complete system in terms of Jy V<sup>-1</sup>. This will depend on the detector responsivity and on other properties of the instrument (e.g., spectral passband, optical efficiency).

### 4.3 Typical parameters for the SPIRE bolometers

In this note we consider a typical SPIRE bolometer, based on the median properties of the PMW detectors, as given in the JPL EIDP spreadsheets:

Parameter	Symbol	Value
Material band-gap temperature	$T_g$	42.1 K
Static thermal conductance at 300 mK	$G_{S_o}$	65.7 pW K <sup>-1</sup>
Resistance parameter	$R_S$	69.5 $\Omega$
Thermal conductivity power law index	$\beta$	1.7
Total load resistance	$R_L$	16.7 M $\Omega$

**Table 1: Typical parameters for a PMW bolometer.**

The load curve (bolometer voltage  $V_{d-RMS}$  vs. current  $I_{b-RMS}$ ) for this typical SPIRE bolometer, with all parameters at their nominal values, is shown in Figure 2. Superimposed is an example load line, determined by the following equation which the bias circuit must satisfy:

$$V_{d-RMS} = V_{b-RMS} - I_{b-RMS} R_L. \quad (14)$$

The bolometer operating point is at the intersection between the load curve and the load line.

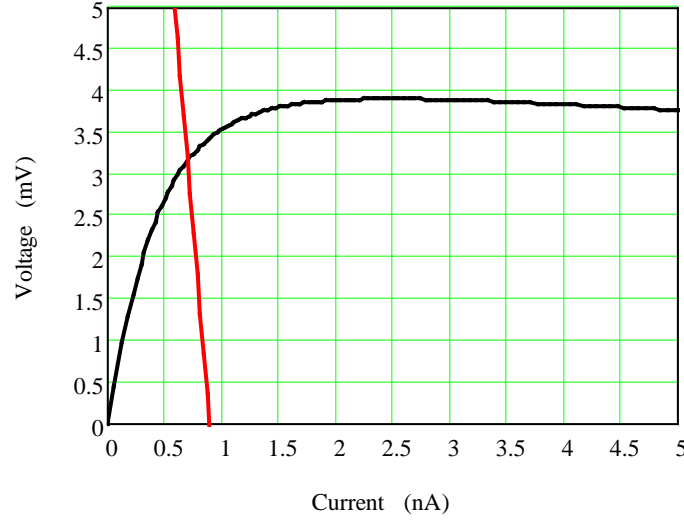


**Figure 2: Load curve and load line for the typical bolometer under nominal operating conditions.**

The bolometer responsivity is defined as

$$S = \frac{dV_{d\text{-RMS}}}{dQ}, \quad (15)$$

and is given by

$$S(\omega_s) = \left[ \frac{Z_d - R_d}{2V_d} \right] \left[ \frac{R_L}{R_L + R_d} \right] \left| \frac{1}{1 + j\omega_s \tau_{eff}} \right|, \quad (16)$$

where  $\omega_s$  is the frequency of modulation of the radiant power on the bolometer,  $Z_d$  is the dynamic impedance of the bolometer ( $dV_d/dI_d$ ) at the operating point,  $\tau_{eff}$  is the effective time constant, defining the first-order response of the bolometer to a step change in radiant power, and the other symbols are as defined above.

If the bolometer signals are at low frequencies such that  $\omega_s \tau_{eff} \ll 1$ , then the responsivity is approximated by the DC value

$$S_o = \left[ \frac{Z_d - R_d}{2V_{d\text{-RMS}}} \right] \left[ \frac{R_L}{R_L + R_d} \right] \quad (17)$$

The DC responsivity varies with the operating point in a manner illustrated by the responsivity-bias curve for the typical SPIRE bolometer, as shown in Figure 3. The peak responsivity occurs at a bias point somewhat before the turn-over in the load curve.

For a small DC increment in radiant power of  $\Delta Q$ , the corresponding increment in the voltage at the bolometer output is

$$\Delta V_{d\text{-RMS}} = S_o \Delta Q \quad (18)$$

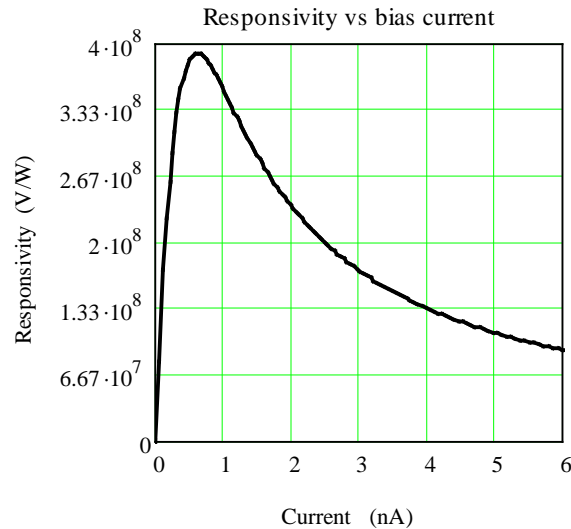


**Figure 3: DC responsivity vs. bias current for the typical bolometer.**

In the event of a step increase in the signal power,  $Q_s$ , the bolometer output will settle to the corresponding equilibrium value following a first-order transient response curve dictated by  $\tau_{eff}$ :

$$\Delta V_{d-RMS}(t) = \Delta V_{d-RMS} \left( 1 - e^{-\frac{t}{\tau_{eff}}} \right). \quad (19)$$

It is important to note that the responsivity is only defined for small deviations about a particular operating point. If the change in  $Q$  is large enough to move the operating point significantly, then using the responsivity will produce an overestimate of the change in output voltage. This non-linear response is considered quantitatively for a typical SPIRE bolometer in Section 5.3.

## 5. Sensitivity of bolometer output and responsivity to operating parameters

For SPIRE, the following parameters could vary during an observation, or between one observation and another.

$Q_s$ , the power absorbed from the astronomical sky - this is what the system is designed to measure;

$T_o$ , the heat sink temperature - ideally this should be constant but in practice there will be fluctuations causing corresponding fluctuations in the detector outputs;

$Q_B$ , the background power from the telescope and other Herschel or SPIRE elements: ideally this should be constant, but in practice there may be fluctuations due to thermal drifts in the system;

$V_{b-RMS}$ , the applied bias voltage: this is expected to be effectively constant for one observation but might be changed between observations in some special cases.

Changes in these parameters will lead to changes in the bolometer operating parameters (voltage, resistance, temperature) and to the responsivity. Changes in the bolometer noise will also occur, but are not considered in this note.

In this section, we quantify the sensitivity of the SPIRE bolometers to changes in these parameters, taking the nominal PMW bolometer as an example. In each case, the bolometer model is used to evaluate the change,

keeping all other parameters at their nominal values, and assuming that the timescale of variation is long compared to the bolometer time constant. The nominal operating conditions are summarised in Table 2. The bolometer is assumed to be biased optimally for the nominal operating conditions, and the applied bias voltage kept constant throughout (except when sensitivity to a change in the actual bias voltage is being considered).

Parameter	Symbol	Value
Heat sink temperature	$T_o$	310 mK
Background power	$Q_B$	1.0 pW
Signal power	$Q_s$	0 pW
RMS bias voltage	$V_{b-RMS}$	15 mV
RMS bolometer voltage	$V_{d-RMS}$	2.91 mV
Bias current	$I_{b-RMS}$	0.72 nA
Bolometer resistance	$R_d$	4.02 M $\Omega$
Bolometer temperature	$T$	350 mK
DC responsivity	$S_o$	348 MV W <sup>-1</sup>

**Table 2: Nominal operating conditions for evaluating sensitivity to changes in bolometer parameters.**

### 5.1 Sensitivity to bath temperature

The impact of varying  $T_o$  over the range 290 – 335 mK was examined and the effects on the load curve and responsivity are shown in Figure 4.

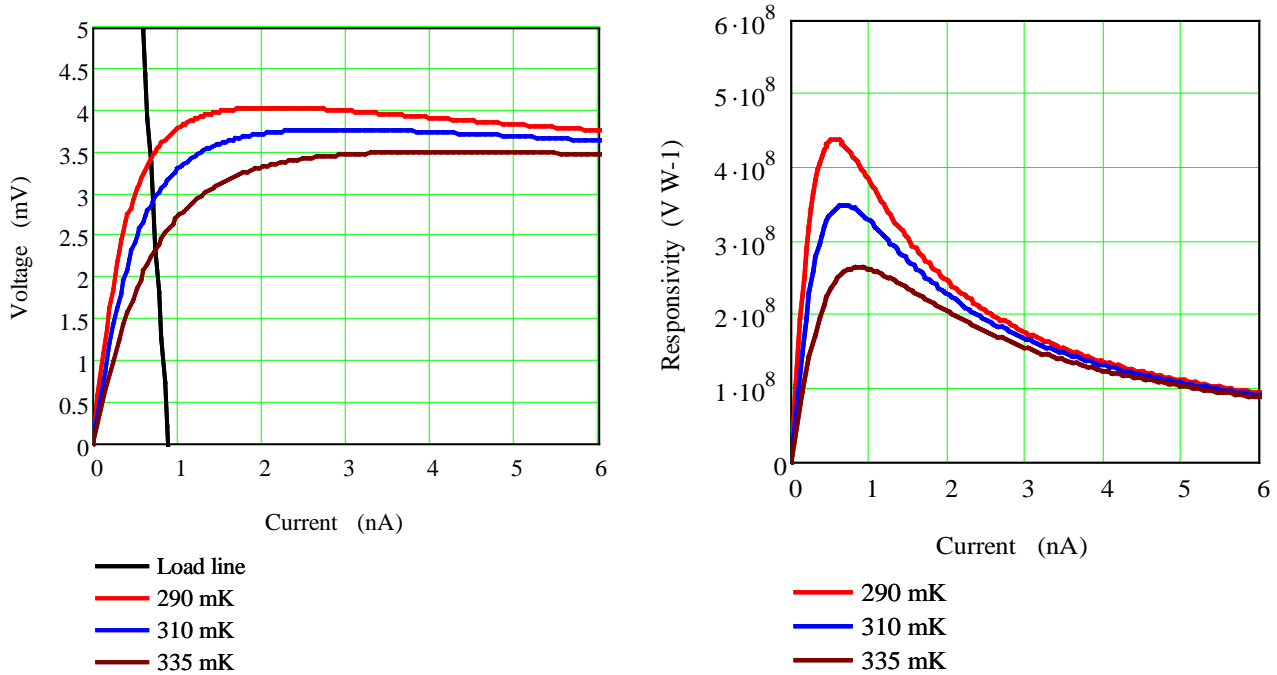


**Figure 4: Effect of change in bath temperature,  $T_o$ , on the load curve (left) and small-signal responsivity (right).**

The normalised responsivity and resistance as a function of  $T_o$  are shown in Figure 5. The variation of both parameters is seen to be nearly linear, with approximately a 1% change per 1 mK change in the heat sink temperature.



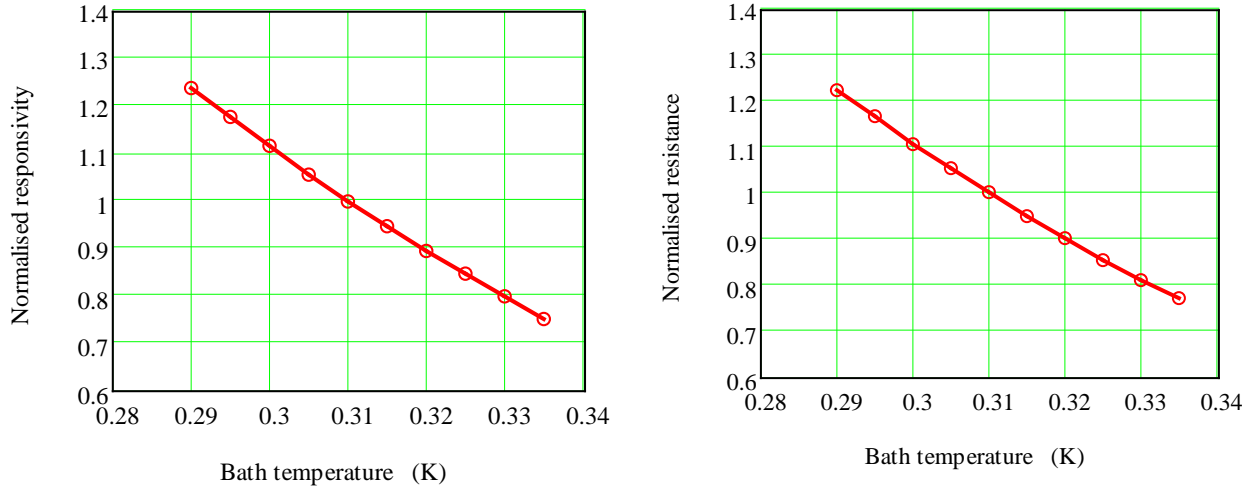


**Figure 5: Effect of change in bath temperature,  $T_o$ , on the normalised responsivity (left) and normalised resistance (right).**

The sensitivity of the operating point voltage to  $T_o$  is shown in Figure 6. The variation is again very linear, with a slope of approximately  $26 \mu\text{V mK}^{-1}$ . With a typical noise voltage spectral density of  $30 \text{ nV Hz}^{-1/2}$  and 5 Hz electrical bandwidth, the bolometer RMS noise voltage is about 67 nV. The  $\Delta T_o$  which would produce a drift equivalent to this noise voltage is about  $2.6 \mu\text{K}$ .

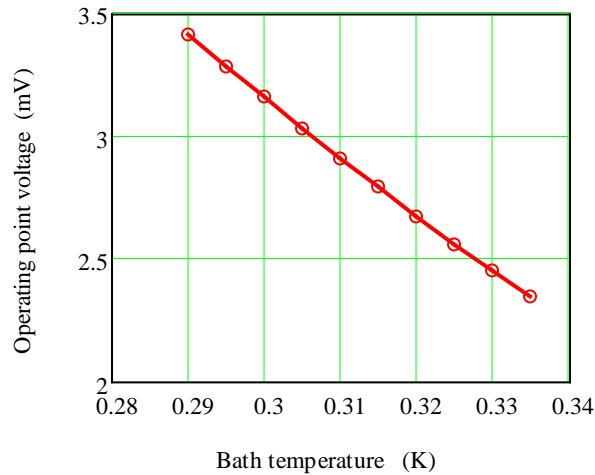


**Figure 6: Effect of change in bath temperature on the bolometer operating point voltage.**

## 5.2 Sensitivity to background power

The impact of varying  $Q_B$  over the range 1.0 – 3.0 pW was examined (recall, 1.0 pW is the nominal telescope background). The load curves and small-signal responsivity curves are shown in Figure 7 and the normalised responsivity and resistance are shown in Figure 8 as a function of  $Q_B$ .

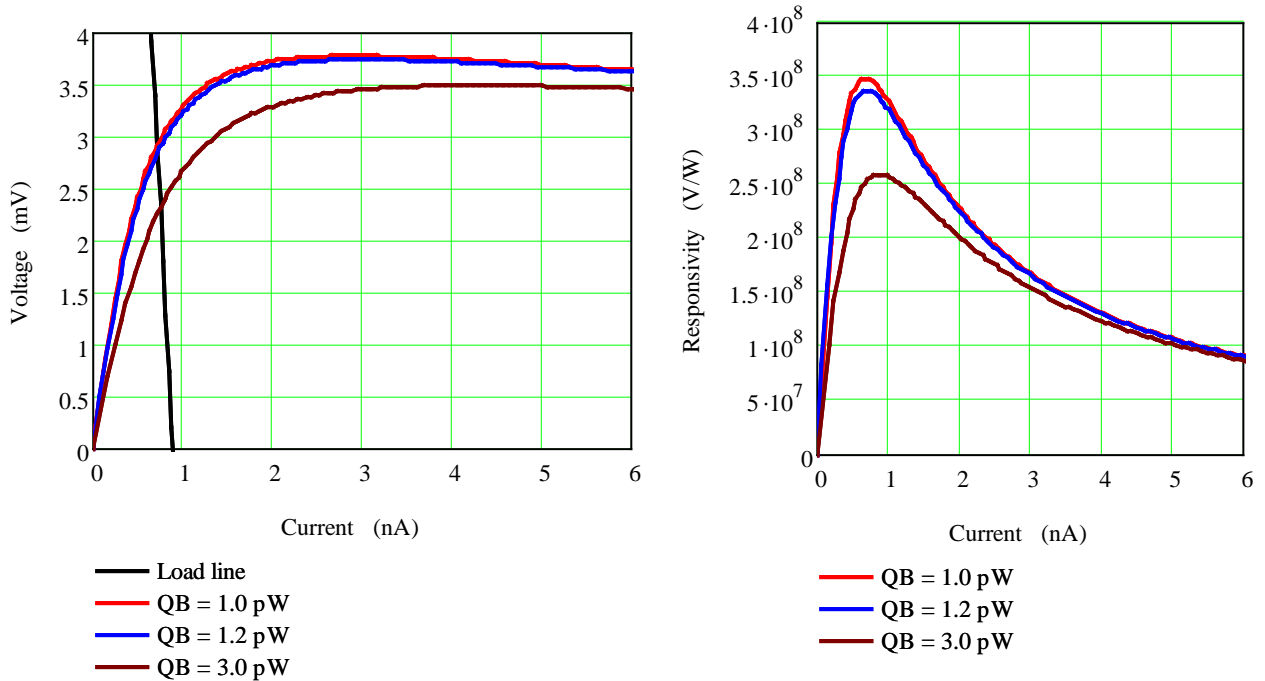


**Figure 7: Effect of change in background power,  $Q_B$ , on the load curve (left) and small-signal responsivity (right).**

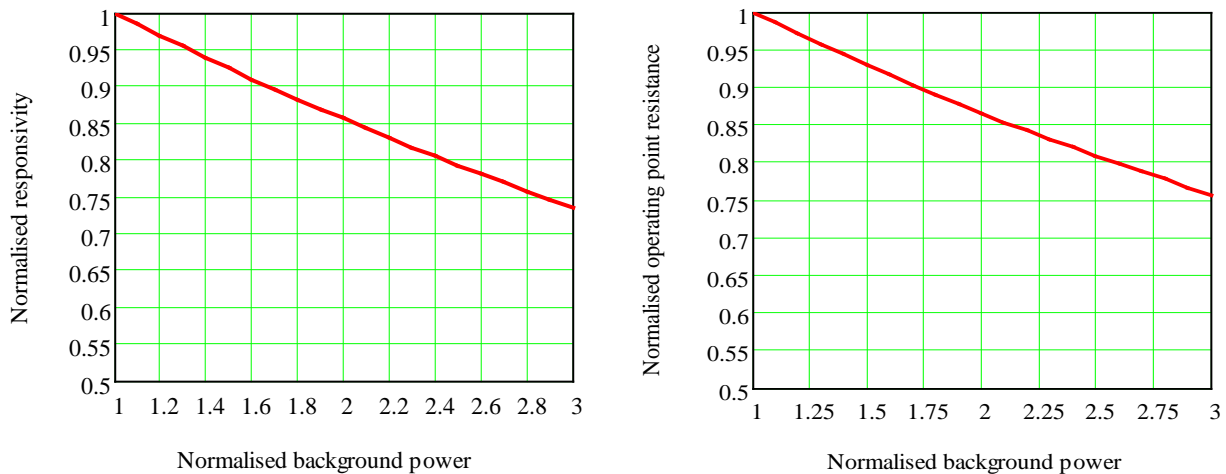


**Figure 8: Effect of change in background power, on the normalised responsivity (left) and normalised operating point resistance (right).**

A 10% change in absorbed power produces change of approximately 1.5% in both small-signal responsivity and operating point resistance. Note that this is true regardless of whether the change is in the telescope background or in the power from the sky.

The sensitivity of the operating point voltage to  $Q_B$  is shown in Figure 9. The variation is again very linear, with a slope of approximately  $0.35 \text{ mV pW}^{-1}$ . [Implications for offset setting to be discussed.](#)

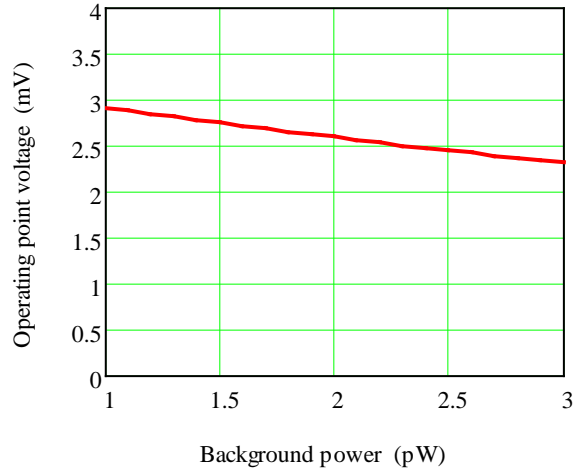


**Figure 9: Effect of change in background power on the bolometer operating point voltage**

### 5.3 Sensitivity to signal power

For small signals, the change in the output voltage is simply given by the responsivity multiplied by the signal power. However, when the signal power is a significant fraction of the background power, the change in the bolometer operating point between the two conditions ( $Q_{\text{tot}} = Q_{\text{B}}$  and  $Q_{\text{tot}} = Q_{\text{B}} + Q_{\text{s}}$ ) is such that the small-signal approximation breaks down. The telescope background power and corresponding source flux density levels for the three bands are:

$$\begin{aligned} \text{PSW} & 1.7 \text{ pW} \equiv 230 \text{ Jy}; \\ \text{PMW} & 1.0 \text{ pW} \equiv 250 \text{ Jy}; \\ \text{PSW} & 1.2 \text{ pW} \equiv 270 \text{ Jy}. \end{aligned}$$

To assess the non-linear response to a bright source, we model the change in output voltage as a function of signal power by explicitly calculating the load curves for the two conditions and determining directly the change in output voltage from the intersection points with the load line.

The operating point voltage and resistance for  $Q_{\text{tot}} = Q_{\text{B}} + Q_{\text{s}}$  are plotted in Figure 10 for the nominal SPIRE bolometer, over the range  $Q_{\text{s}} = 0 - 3 \text{ pW}$  (with the upper end of the range corresponding to a signal power three times larger than the telescope background).

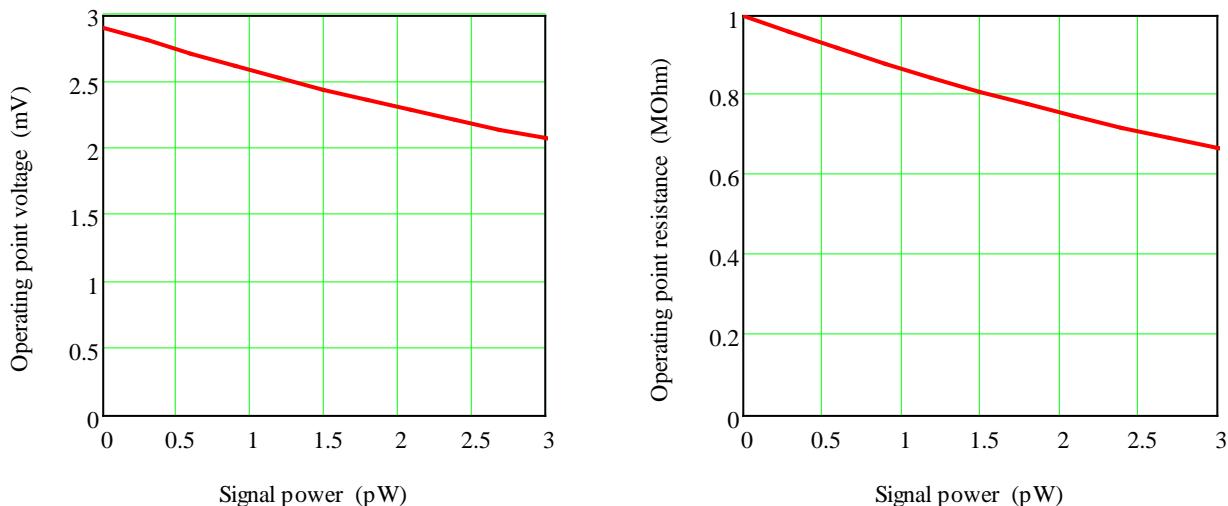


**Figure 10: Effect of change in signal power,  $Q_{\text{s}}$ , on the operating voltage (left) and resistance (right).**

The resistance changes by about 13% per pW of signal power. The response of the operating point voltage is best presented in the form of the measured change,  $\Delta V_{d-RMS}(\text{measured})$ , with respect to the operating point for zero signal – i.e., the measured signal voltage. This is shown in Figure 11. The left panel shows the measured signal voltage compared with the ideal value (based on the small signal responsivity). The departure from the linear behaviour can be accurately characterised by a second-order polynomial. The same information is depicted in the right-hand panel, which shows the fractional non-linearity of the measured signal as a function of normalised signal power (the non-linearity is defined as  $\Delta V_{d-RMS}(\text{measured})/\Delta V_{d-RMS}(\text{ideal})$ )

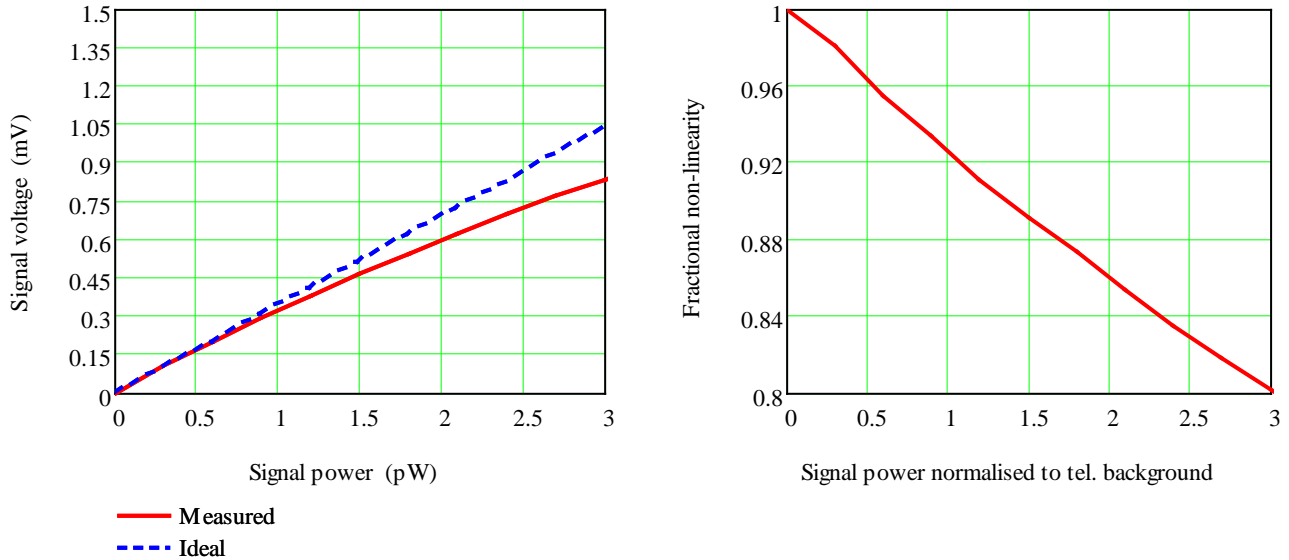


**Figure 11: Signal voltage vs. signal power (left); fractional non-linearity vs. signal power normalised to the telescope emission.**

We see that for the PMW detector

- a signal comparable to the telescope background results in about 8% non-linearity;
- a signal of about 30% of the telescope ( $\sim 80$  Jy) produces a 2% non-linearity;
- the degree of non-linearity is approximately linearly proportional to the signal power.

#### 5.4 Sensitivity to bias voltage

One possibility for coping with extremely strong sources is to decrease the bolometer responsivity by changing the bias voltage. The variation of responsivity with bias voltage is shown in Figure 12.

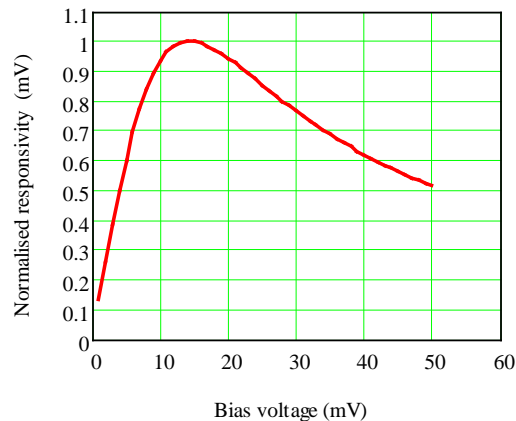


**Figure 12: Variation of responsivity with bias voltage for the nominal PMW bolometer.**

It can be seen that overbiasing the bolometer even by a significant amount does not result in a large decrease, but underbiasing can reduce the responsivity by a large amount. However, the sensitivity of the responsivity to any fluctuations in the various parameters will also be higher than at the nominal settings.

### 5.5 Relationship between responsivity and operating point voltage

Figure 13 shows the responsivity as a function of the operating point voltage for signal power. The variation is approximately linear relationship over a wide range of signal power – up to several times the brightness of the telescope. This translates to a corresponding relationship between the differential sensitivity of the system to astronomical source flux density and the operating point voltage (which is measured directly by the SPIRE data-sampling system).

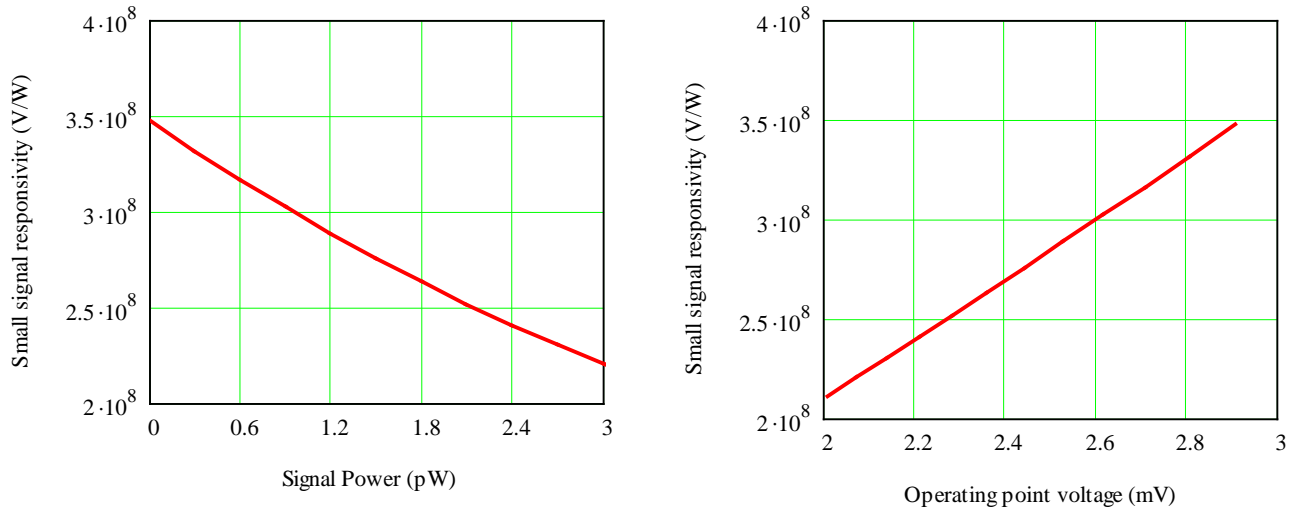


**Figure 13: Variation of DC responsivity with signal power (left) and corresponding operating point voltage (right) for the typical PMW detector.**

The operating point voltage can be used as a way of tracking the responsivity, and this will allow large signals to be calibrated by integrating the relationship, as described in *The SPIRE Analogue Signal Chain and Photometer Detector Data Processing Pipeline* (Griffin, 2007).

## 6. References

Griffin, M. The SPIRE Analogue Signal Chain and Photometer Detector Data Processing Pipeline. *SPIRE-UCF-DOC-002890*, Issue 1.0, June 8 2007.

Mather J C. Bolometer noise: nonequilibrium theory. *Applied Optics* 21, 1125, 1982.

Sudiwala R V, M J Griffin, and A L Woodcraft. Thermal modelling and characterisation of semiconductor bolometers. *Int. J. Infrared. Mm. Waves*, 23, 575, 2002.